

# Dynamically Amplified Rate Integrating Gyroscopes

C. Painter and A. Shkel

Microsystems Laboratory  
Department of Mechanical and Aerospace Engineering  
University of California, Irvine  
4200 Engineering Gateway, Irvine, CA 92612  
cpainter@uci.edu, ashkel@uci.edu, <http://mems.eng.uci.edu>

## ABSTRACT

A novel micromachined rate integrating gyroscope using a dual mass architecture is proposed which is capable of measuring angular positions rather than angular rates. The proposed device decouples drive and sense modes of operation by using an active mass exclusively for drive and control and a second, passive mass, exclusively for sense. Additionally, the passive mass is made to vibrate at large amplitudes of motion, facilitating high sense capabilities, while the drive mass retains small amplitudes of motion, operating in a linear capacitive region. In this paper, we present the principles of operation of the device and a novel control architecture which allows the device to work in rate integration mode while simultaneously achieving dynamic amplification. Simulations based off parameters of a fabricated device demonstrate the angle sensing capabilities.

**Keywords:** Rate Integrating Gyroscopes, MEMS, Dynamic Amplification, Dual Mass

## 1 INTRODUCTION

As MEMS based inertial sensors have been slowly proliferating into the market over the past decades, the challenge for MEMS gyroscope designers has been to create sensors with both high performance and low cost. There is a lack of low cost, MEMS based gyroscopes on the market capable of navigation grade inertial sensing, mainly due to inadequate drift and noise performance. Thus, one potential source of large attitude errors arises from integration of the rate signal to obtain orientation. One proposed solution addressing this problem is the development of MEMS based gyroscopes capable of directly sensing orientation, or rate integrating gyroscopes. MEMS rate integrating gyroscopes based on vibrating rings [1] and vibrating masses [2] have been earlier proposed, which both require nonlinear electrostatic parallel plates for actuation and sensing. The challenge in these devices is that large amplitudes of motion are desirable for larger amplitudes of sensing, which at the same time result in a higher degree of nonlinearity, making it difficult to apply control algorithms for drive and error suppression. Our solution to this challenge is a dual mass system where an active mass is used exclu-

sively for drive and control and the second coupled, passive mass is used exclusively for sensing motion. With an appropriate choice of geometry, the actively driven mass can operate with a small range of motion so as to maintain a linear operating regime while dynamically amplifying the motion of the passive mass to increase sensing capabilities.

Previous work in MEMS under the principles of dynamic amplification has been done in micromachined dual mass rate gyroscopes [3], and more generally in a dual mass resonator device using parallel plate electrodes [4]. However each of these devices uses a one dimensional control, where they need only sustain oscillation along one axis of motion. What separates the proposed device from these designs is that rate integrating gyroscopes start with a line of oscillation initially along one direction, but this line of oscillation must be allowed to precess in the presence of Coriolis force. As a result, the device requires a two dimensional control architecture to maintain the motion of the passive mass assuming that the line of oscillation may be oriented anywhere within a two dimensional working plane.

## 2 DYNAMICS

For a dual mass-spring-damper model (Figure 1a), the equations of motion are

$$\begin{aligned} m_1 \ddot{x}_1 + c_1 \dot{x}_1 + (k_1 + k_2) x_1 - k_2 x_2 - 2m_1 \Omega \dot{y}_1 &= F_x \\ m_1 \ddot{y}_1 + c_1 \dot{y}_1 + (k_1 + k_2) y_1 - k_2 y_2 + 2m_1 \Omega \dot{x}_1 &= F_y \\ m_2 \ddot{x}_2 + c_2 \dot{x}_2 + k_2 x_2 - k_2 x_1 - 2m_2 \Omega \dot{y}_2 &= 0 \\ m_2 \ddot{y}_2 + c_2 \dot{y}_2 + k_2 y_2 - k_2 y_1 + 2m_2 \Omega \dot{x}_2 &= 0 \end{aligned} \quad (1)$$

where  $m_1$  and  $m_2$  and  $c_1$  and  $c_2$  are the mass and damping of the drive and slave mass, respectively. Parameters  $k_1$  and  $k_2$  are the spring constants for the spring attached to the drive mass and the spring coupling the drive and slave mass, respectively.  $F_x$  and  $F_y$  are applied external control forces on the driven mass and  $\Omega$  is a constant input angular rotation. Here, any coupled damping between the masses can be neglected if there is good separation between the drive and slave masses. If damping is sufficiently small and the input angular velocity is orders of magnitude less than the two eigenfrequencies, then both damping and Coriolis forces can be

considered as small, regular perturbations. Thus, time averaging techniques similar to one used for single mass rate integrating gyroscopes [5] can be implemented. In the case of the single mass gyroscopes, the averaging leads to approximations for the long term behavior of the gyroscope in the presence of the imperfections. We shall show that similar results can be obtained in our case of two masses. The first step in this process is to find the homogeneous solution in the absence of perturbations

$$\begin{aligned}
x_i &= M_i a_1 \cos \phi_1 \cos \theta_1 + N_i a_2 \cos \phi_2 \cos \theta_2 \\
&\quad - M_i b_1 \sin \phi_1 \sin \theta_1 - N_i b_2 \sin \phi_2 \sin \theta_2 \\
y_i &= M_i a_1 \sin \phi_1 \cos \theta_1 + N_i a_2 \sin \phi_2 \cos \theta_2 \\
&\quad M_i b_1 \cos \phi_1 \sin \theta_1 - N_i b_2 \cos \phi_2 \sin \theta_2 \quad (2) \\
i &= 1, 2 \\
\theta_1 &= e_1 t + \gamma_1 \\
\theta_2 &= e_2 t + \gamma_2
\end{aligned}$$

where  $i$  are indices corresponding to the drive and slave masses,  $M_1$ ,  $M_2$ ,  $N_1$ , and  $N_2$  are constant functions of the structural parameters  $k_1$ ,  $k_2$ ,  $m_1$ , and  $m_2$  and  $e_1$  and  $e_2$  are the two eigenfrequencies (Figure 1b). Letting  $u = \{x_1, y_1, x_2, y_2, \dot{x}_1, \dot{y}_1, \dot{x}_2, \dot{y}_2\}$  and  $z = \{a_1, b_1, \phi_1, \gamma_1, a_2, b_2, \phi_2, \gamma_2\}$ , the homogeneous solution can be expressed as  $u = g(z)$ . Here, variables  $\{x_1, y_1\}$  and  $\{x_2, y_2\}$  define quasi elliptical trajectories of the two masses where constants  $a_1$ ,  $a_2$ ,  $b_1$ , and  $b_2$  are initial condition determined constants which define the general shape of the elliptical trajectories,  $\phi_1$  and  $\phi_2$  are constants defining the orientation of the two mass trajectories, and constants  $\gamma_1$  and  $\gamma_2$  designate the initial position of each mass on its trajectory. Under the assumption that  $a_1$ ,  $a_2$ ,  $b_1$ ,  $b_2$ ,  $\phi_1$ , and  $\phi_2$  change slowly in one period of oscillation in the presence of small perturbations  $f(u)$ , the second and third steps in the procedure are to write the dynamic system in terms of the changing constants and then perform averaging over a period of oscillation [5]

$$\dot{z} \approx \frac{1}{T} \int_0^T J^{-1} h(z, t) dt$$

where  $T = 2\pi/\omega$  and  $h = f(g(z, t))$ . Parameter  $\omega$  is the frequency of oscillation, which complicates the averaging procedure as there are two different periods of oscillation. However, if the perturbations are purely Coriolis force, then  $\dot{z}$  decouples into exclusively  $e_1$  components for the drive mass variables and  $e_2$  components for the slave mass variables. Thus,  $\omega = e_1$  for  $a_1$ ,  $b_1$ , and  $\phi_1$  and  $\omega = e_2$  for  $a_2$ ,  $b_2$ , and  $\phi_2$ . Equation (3) gives the dynamics with respect to the slow changing variables as

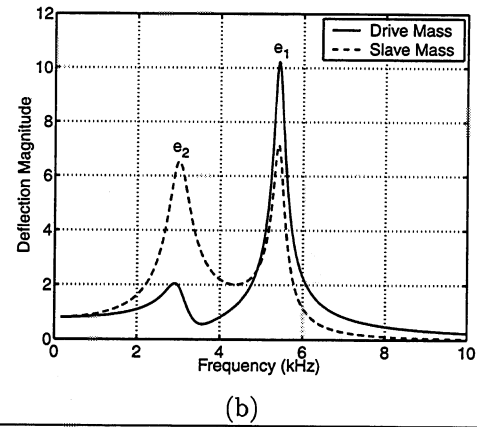
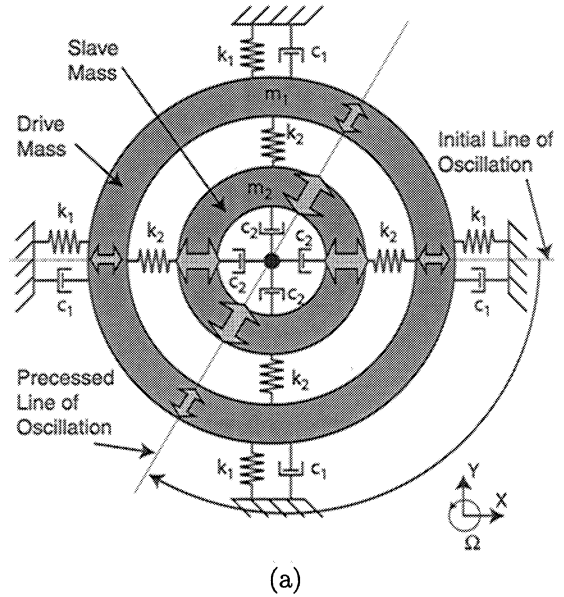


Figure 1: (a) Model of the coupled dual mass-spring dynamical system. (b) Frequency response of a dual mass-spring system. By actuating the drive mass at the first resonant frequency ( $e_2$ ), we can achieve large amplitude deflections in the slave mass while retaining small deflections in the drive mass.

$$\begin{aligned}
\dot{a}_1 &\approx 0 & \dot{a}_2 &\approx 0 \\
\dot{b}_1 &\approx 0 & \dot{b}_2 &\approx 0 \\
\dot{\phi}_1 &\approx -\Omega & \dot{\phi}_2 &\approx -\Omega
\end{aligned} \quad (3)$$

We see that the angle  $\phi_2$  is equal to the negative angular deflection

$$\phi_2 = - \int_0^t \Omega dt \quad (4)$$

Thus, in our dynamic system, if  $\phi_2$  can be instantly identified from sense electronics, the angular deflection of the device can be measured.

## 2.1 Sense and Drive

Since the goal of the device is to decouple drive and sense functionality, it is desirable to calculate precession

from only the slave mass position and velocity and apply forces only on the active mass. From Equation (2) we see the the slave mass position is comprised of two frequency components,  $e_1$  and  $e_2$ . If there is good separation between the eigenfrequencies, we can assume that the position and velocity can be demodulated into components of the two frequencies. Assume that we now have the following demodulated positions and velocities

$$\begin{aligned}\tilde{x}_2 &= \frac{1}{n} a_2 \cos \phi_2 \cos \theta_2 - \frac{1}{n} b_2 \sin \phi_2 \sin \theta_2 \\ \tilde{y}_2 &= \frac{1}{n} a_2 \sin \phi_2 \cos \theta_2 - \frac{1}{n} b_2 \cos \phi_2 \sin \theta_2 \\ \dot{\tilde{x}}_2 &= -\frac{1}{n} a_2 e_2 \cos \phi_2 \sin \theta_2 - \frac{1}{n} e_2 b_2 \sin \phi_2 \cos \theta_2 \\ \dot{\tilde{y}}_2 &= -\frac{1}{n} a_2 e_2 \sin \phi_2 \sin \theta_2 - \frac{1}{n} b_2 e_2 \cos \phi_2 \cos \theta_2\end{aligned}\quad (5)$$

From here, the precession angle  $\phi_2$ , which was determined to be proportional to the angular displacement, can be instantly identified as

$$\tan 2\phi_2 = \frac{2(e_2^2 \tilde{x}_2 \dot{\tilde{y}}_2 + \dot{\tilde{x}}_2 \tilde{y}_2)}{e_2^2 (\tilde{x}_2^2 - \dot{\tilde{y}}_2^2) + (\dot{\tilde{x}}_2^2 - \tilde{y}_2^2)} \quad (6)$$

In order to drive the system to a steady energy state, an energy compensating feedback control similar to one used in single mass rate integrating gyroscopes [6] is proposed

$$\begin{aligned}F_x &= -\kappa \cdot \Delta E \cdot \dot{\tilde{x}}_2 \\ F_y &= -\kappa \cdot \Delta E \cdot \dot{\tilde{y}}_2\end{aligned}\quad (7)$$

where  $\kappa$  is a gain and  $\Delta E$  is the difference between a user defined nominal energy  $E_0$  and the instantaneous total energy of the slave mass  $E(t)$ . Under this control, the drive frequency is always the lower eigenfrequency  $e_2$ , resulting in dynamic amplification of the slave mass (see Figure 1b).

### 3 SIMULATION

The dynamic system from Equation (1) is modeled using parameters based off a fabricated surface micromachined device (Figure 2). Here,  $m_1 = 4.44 \times 10^{-10}$  kg,  $m_2 = 5.20 \times 10^{-10}$  kg,  $k_1 = 4.0$  N/m, and  $k_2 = 0.25$  N/m. To illustrate the precession of the oscillation pattern, the device is first run with no damping ( $c_1 = c_2 = 0$ ) at an angular velocity  $\Omega = 200$  rad/sec. Plots of the drive mass and slave mass positions (Figure 3a) show that the oscillation pattern of each mass precesses identically. To demonstrate the amplification capabilities of the controller, the simulation is run with small damping introduced ( $c_1 = c_2 = 1.933 \times 10^{-8}$  (N · sec)/m) and an

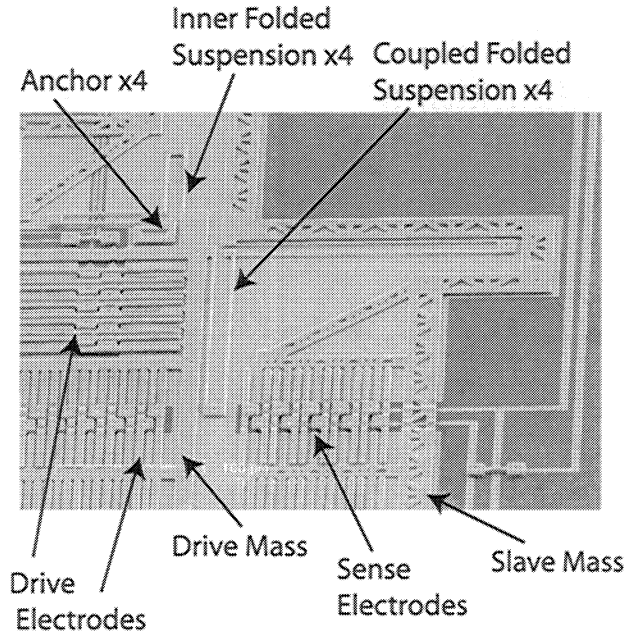


Figure 2: A prototype surface micromachined rate integrating gyroscope using a dual mass architecture. Folded suspensions serve as the spring members and electrostatic parallel plates are used for drive and sense.

input angular velocity of 1 rad/sec over a time period of 1 sec. Demodulation of the slave mass position is performed using a low pass filter with a cutoff frequency of 8 kHz, roughly halfway between the two eigenfrequencies ( $e_2 = 3.5$  kHz and  $e_1 = 15.5$  kHz). The demodulated slave position is then used to calculate the precession angle with respect to the moving frame based off Equation (6). The demodulated slave position is also fed back to the drive mass through the energy compensating controller of the same architecture as Equation (7). The plot of the output precession angle (Figure 3b) shows an output of -1 radians (the actual angular deflection is the opposite sign as the precession angle). In addition, the control achieves dynamic amplification with an over tenfold amplification of the passive mass deflection over the active mass deflection (Figure 3c).

### 4 CONCLUSION

In this paper, we have proposed a novel rate integrating gyroscope design using a dual mass architecture as a way to decouple drive and sense functionality. We have shown analytically and through simulation that the line of oscillation of a dual mass device operating under ideal operating conditions precesses at the same rate as an input angular velocity. We have shown that the precession angle equal to the angle of rotation can be calculated from the output position and velocity of the slave mass. An energy compensating controller was demonstrated which feedbacks motion from the slave mass to apply forces on the drive mass. Through simu-

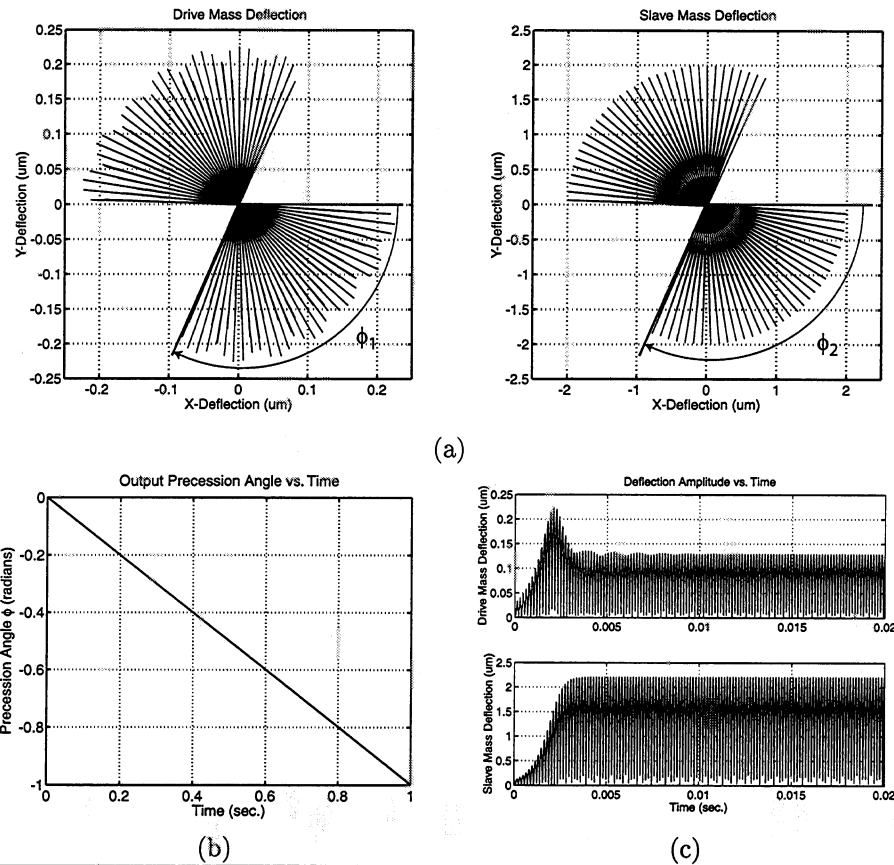


Figure 3: (a) For illustrative purposes, the simulation is run for .01 sec with an input angular velocity of 200 rad/sec, zero damping, and no feedback control. The line of oscillation of each mass is observed to precess identically with high amplitudes of motion in the passive mass compared to the active mass. (b) Simulation is then run for 1 sec. with an input angular velocity of 1 rad/sec, small damping, and the energy compensating control. The measured precession angle is -1 rad, exactly equal to the negative angular deflection of the device. (c) From the plots of the deflection magnitude between the slave and drive mass, there is an over ten fold amplification in motion.

lation using parameters based off a realistic implementation of the device, the controller was demonstrated to dynamically amplify the motion of the slave mass with respect to the driven mass without interfering with the precession. Future work includes analyzing the effect of non-idealities such as anisotropy and coupled damping on the performance of such a device, implementation of compensating control methods, and experimental demonstration of the device.

## 5 ACKNOWLEDGEMENTS

The author would like to thank the Department of Defense who is sponsoring this work through a 2001 National Defense Science and Engineering Graduate Fellowship.

## REFERENCES

[1] M. Putty, and K. Najafi. A Micromachined Vibrating Ring Gyroscope. In *IEEE Solid State Sen-*

*sors and Actuators Workshop*, pages 213–220, Hilton Head Island, SC, June 1994.  
 [2] A. Shkel and R. T. Howe. Polysilicon surface micro-machined rate integrating gyroscopes. UC-Berkeley Office of Technology and Licensing. Case Number B99-077.  
 [3] C. Acar and A. Shkel. Wide bandwidth micromachined gyroscope to measure angular rotation. UCI Case Number: 2001-140-1.  
 [4] C. Dyck, J. Allen and R. Huber. Microelectromechanical dual-mass resonator structure, May 2002. U.S. Patent 6,393,913.  
 [5] B. Friedland and M. Hutton. Theory and error analysis of vibrating-member gyroscope. *IEEE Transactions on Automatic Control*, AC-23(4):545–556, 1978.  
 [6] A. Shkel, R. Horowitz, A. Seshia, and R.T. Howe. Dynamics and control of micromachined gyroscopes. In *The American Control Conference*, pages 2119–2124, San Diego, CA, June 1999.